

## Engineering Conferences International ECI Digital Archives

---

10th International Conference on Circulating  
Fluidized Beds and Fluidization Technology -  
CFB-10

Refereed Proceedings

---

Spring 5-5-2011

# DEM Study of Fluidized Bed Dynamics During Particle Coating in a Spouted Bed Apparatus

Sergiy Antonyuk

*Hamburg University of Technology*, [antonyuk@tuhh.de](mailto:antonyuk@tuhh.de)

Stefan Heinrich

*Hamburg University of Technology*, [stefan.heinrich@tuhh.de](mailto:stefan.heinrich@tuhh.de)

A. Ershova

*Hamburg University of Technology*

Follow this and additional works at: <http://dc.engconfintl.org/cfb10>

 Part of the [Chemical Engineering Commons](http://dc.engconfintl.org/cfb10)

---

### Recommended Citation

Sergiy Antonyuk, Stefan Heinrich, and A. Ershova, "DEM Study of Fluidized Bed Dynamics During Particle Coating in a Spouted Bed Apparatus" in "10th International Conference on Circulating Fluidized Beds and Fluidization Technology - CFB-10", T. Knowlton, PSRI Eds, ECI Symposium Series, (2013). <http://dc.engconfintl.org/cfb10/89>

This Conference Proceeding is brought to you for free and open access by the Refereed Proceedings at ECI Digital Archives. It has been accepted for inclusion in 10th International Conference on Circulating Fluidized Beds and Fluidization Technology - CFB-10 by an authorized administrator of ECI Digital Archives. For more information, please contact [franco@bepress.com](mailto:franco@bepress.com).

# DEM STUDY OF FLUIDIZED BED DYNAMICS DURING PARTICLE COATING IN A SPOUTED BED APPARATUS

Sergiy Antonyuk, Stefan Heinrich, Anastasia Ershova  
Institute of Solids Process Engineering and Particle Technology, Hamburg  
University of Technology, Denickestrasse 15, 21073 Hamburg, Germany  
T: +49-40-42878-2748; F: +49-40-42878-2678; E: [antonyuk@tu-harburg.de](mailto:antonyuk@tu-harburg.de)

## ABSTRACT

A novel process for coating of spherical aerogel particles in a spouted bed is suggested. Using Discrete Element Method the influence of the density and restitution coefficient of experimentally coated aerogels on the fluidized bed dynamics in the developed apparatus was described.

## INTRODUCTION

The aerogels are nanoporous materials which show extremely low density, high surface area and excellent insulation properties. However, the limitation of aerogels in a number of applications is their open-pore structure, allowing the penetration of liquids therein. Their structure might be destroyed by contact with water because of capillary forces which are higher than the strength (Antonyuk et al. (1)). This drawback could be overcome by coating of aerogels with a polymeric protection material. In this work the aerogel particles were coated in a spouted bed apparatus. This technology offers the fluidization of small and light or very large particles, which can be non-spherical or sticky with a broad size distribution, Mörl et al. (2).

One objective of this work was to produce the coated aerogel particles with good structural properties. In order to optimize the coating process parameters the particle and fluid dynamics of spouted bed apparatus was investigated by Discrete Element Method (DEM) which is coupled with CFD.

## EXPERIMENTAL

### Experimental Slit-shaped Spouted Fluidized Bed

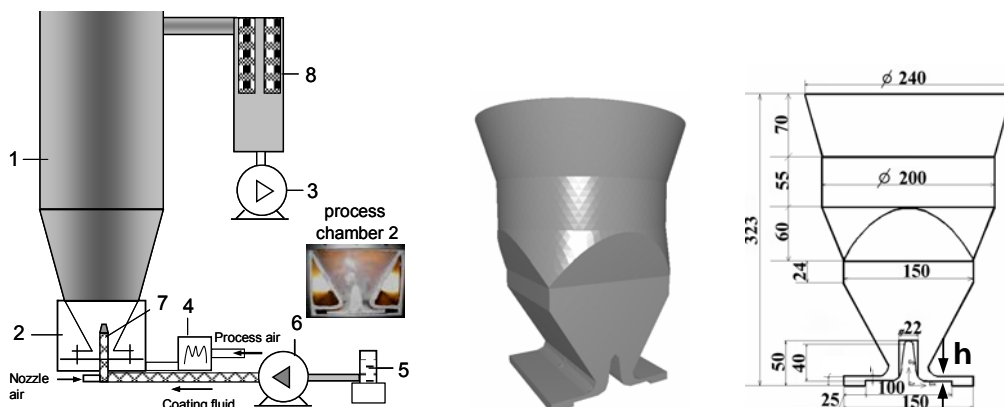


Fig. 1 Experimental spouted bed apparatus for the coating of aerogels (left) and its fluidization chamber (middle and right).

To perform the coating of the aerogels an experimental spouted bed apparatus was built, Fig. 1, which allows an operation under batch conditions. The pilot plant has a cylindrical chamber, Item 1, which is connected through a conic part with a prismatic fluidization chamber, Item 2, with two horizontal gas inlets (slots) for adjustable gas supply. The velocity of the inlet air can be varied changing the height of these slots  $h$ . The air flow produced from blower, Item 3, can be heated up to 100 °C in a 500 W heater, Item 4. The solution or melt prepared in the vessel, Item 5, was transported in a coated hose using a peristaltic pump, Item 6, and injected in the fluidized bed using a two-component nozzle 7. The nozzle was heated up to temperature of injecting fluid. A fabric filter, Item 8, separates small particles from the exhaust gas. The air temperatures before, after and inside the bed (chamber 2), the temperatures of the liquid and nozzle and pressure drop were measured.

### Materials for the Coating Experiments

Fig. 2 shows nearly spherical silica aerogels produced by supercritical extraction of a gel-oil emulsion (Alnaief&Smirnova (3)). The particles with the size ranging from 100  $\mu\text{m}$  to few millimetres and the mean density of 190  $\text{kg}/\text{m}^3$  were coated with Eudragit<sup>®</sup> (solution with 25.8 vol-% of the solid material) which provides a pH sensitive release of the drugs.

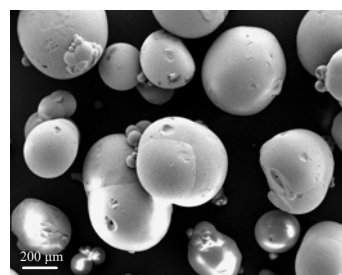


Fig. 2 SEM of produced silica aerogel particles.

### Parameter and Results of the Coating Experiments

During the first experiments the high shrinking of aerogels was observed. The droplets of Eudragit solution destroyed the particle surface of aerogel and their size decreased (Antonyuk et al. (1)). The Eudragit layer showed many cracks (Fig. 3). Hence, to avert the breaking of the particles the coating with two materials was carried out. Firstly the PEG 2000 was sprayed in the apparatus forming a protection layer on the aerogel. Thereafter the Eudragit<sup>®</sup> was injected (Fig. 4). The different process parameters were varied during coating experiments and their optimal values were obtained, which are summarised in Table 1.

Table 1. Process parameters of the coating.

Parameter	PEG 2000	Eudragit <sup>®</sup> L
process air mass flow in $\text{m}^3/\text{h}$	25-40	25-40
bed temperature in °C	45	21
mass flow of the coating fluid in g/min	20	10
temperature of the coating fluid in °C	95	25
flow rate of the nozzle air in l/min	15-20	15-20
temperature of the nozzle in °C	80	30

### Mechanical Properties of the Aerogels

The mechanical properties characterize the product quality. They are also important parameters in the calculated here DEM model (Antonyuk et al. (4)). The stiffness and breakage properties of aerogel were measured by compression tests (Antonyuk et al. (1)) and presented in Table 2 for the different sizes (uncoated particles with  $d_{50} = 0.7 \text{ mm}$  and two fractions of coated particles with  $d_{50} = 0.8 \text{ mm}$  and  $3.71 \text{ mm}$  with layer thickness of approximately  $50 \mu\text{m}$ ).

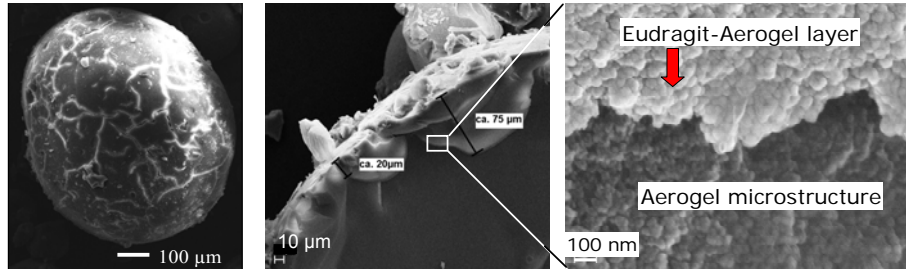


Fig. 3 Aerogel particle coated in spouted bed apparatus with Eudragit® L solutions (left) and the cross section area of the layer (middle and right).

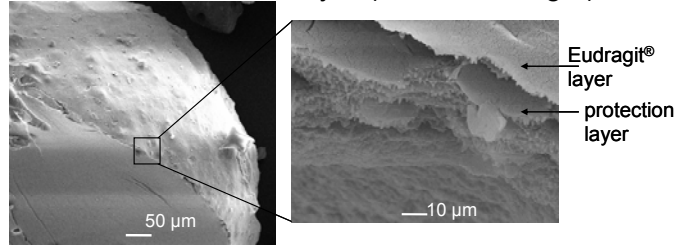


Fig. 4 Cross section area of a silica aerogel particle coated with two layers.

Table 2 Mechanical characteristics of aerogels.

Diameter in mm	Breakage force in N	Strength in kPa	Stiffness in N/mm
0.70 ± 0.14	0.37 ± 0.2	970 ± 0.50	10.3 ± 2.0
0.80 ± 0.12	0.33 ± 0.1	650 ± 460	10.0 ± 3.0
3.71 ± 0.40	0.61 ± 0.2	60 ± 30	3.0 ± 0.6

The aerogels with Eudragit shell show smaller strength in comparison with the uncoated particles. The decreasing of the strength occurs due to damaging of the particle surface by contact with Eudragit®. No significant influence of the shell on the particle stiffness was obtained. With the increasing of the particle size (from 0.8 to 3.7 mm) the strength and stiffness decrease.

The impact and rebound behaviour of aerogels before ( $d_{50} = 1.5$  mm) and after coating ( $d_{50} = 1.7$  mm) was analyzed with the help of a free fall set-up (Antonyuk et al. (8)). The normal coefficients of restitution ( $e_{\text{uncoated}} = 0.6 \pm 0.13$  and  $e_{\text{coated}} = 0.4 \pm 0.16$ ) were measured at the impact velocity range of 1 m/s. They are input parameters for the DEM model, which will be described in the next paragraph.

## MODELLING OF PARTICLE AND FLUID DYNAMICS

### DPM Model

A discrete particle model (DPM) was employed to study the particle and fluid dynamics of spout bed apparatus used for the coating of aerogel. The DPM is a coupling of the discrete element method (DEM), which describes the motion of every individual element, and the computational fluid dynamics (CFD), which calculates the gas phase (van Buijtenen et al. (5), Fries et al. (6)). The motion of each particle  $i$  can completely be described using Newton's and Euler's laws:

$$m_i \frac{d\vec{v}_i}{dt} = -V_i \nabla \bar{p} + \frac{V_i \beta_{g-p}}{1 - \varepsilon} (\vec{u}_g - \vec{v}_i) + m_i \vec{g} + \sum_{j=1}^m \vec{F}_{c,j,i}, \quad (1)$$

$$I_i \frac{d\bar{\omega}_i}{dt} = \sum_{j=1}^l \bar{M}_{i,j}. \quad (2)$$

The force balance on the right side of Eq. (1) consists of the force due to pressure gradient, drag, gravity and contact forces by a particle-particle and particle-wall collision, respectively.  $I_i$  and  $\omega_i$  in Eq. (2) are the moment of inertia and angular velocity for particle  $i$ .  $M_{i,j}$  are the moments generated from tangential contact forces acting on the particle  $i$ . The interphase momentum transfer coefficient  $\beta_{g-p}$  is modelled by combining the Ergun equation (1952) for dense regimes ( $\varepsilon \leq 0.8$ ) and the correlation proposed by Wen&Yu (1966) for more dilute regimes ( $\varepsilon > 0.8$ ).

Contact forces between particles are calculated according to a viscoelastic contact model based on the Kelvin-Voigt law with a constant restitution coefficient (Cundall and Strack (7)). The normal and tangential contact forces are defined as follows:

$$\vec{F}_{c,n}^{(ij)} = (k_{c,ij,n} \cdot s_{ij,n} + \eta_{ij,n} \cdot \dot{s}_{ij,n}) \cdot \vec{n}_{ij}, \quad (3)$$

$$\vec{F}_{c,s}^{(ij)} = \min \left[ \begin{array}{l} (k_{c,ij,s} \cdot s_{ij,s}^a + \eta_{ij,s} \cdot \dot{s}_{ij,s}) \cdot \vec{t}_{ij} \\ (\mu_{ij} \cdot F_{c,n}^{(ij)}) \cdot \vec{t}_{ij} \end{array} \right], \quad (4)$$

where  $k_{c,ij,n}$  and  $k_{c,ij,s}$  are the contact stiffness in normal and shear direction,  $\mu_{ij}$  is the dynamic friction coefficient. The overlap in normal and shear direction is  $s_{ij,n}$  and  $s_{ij,s}$ .  $\eta_{ij,n}$  and  $\eta_{ij,s}$  are the normal and shear damping given as:

$$\eta = \sqrt{4m^* \cdot k_c / \left[ 1 + \left( \frac{\pi}{\ln e} \right) \right]}. \quad (5)$$

$m^*$  is equivalent mass of contact partners.  $k_c$  is the contact stiffness. The coefficient of restitution,  $e$ , describes the energy dissipation during impact and can be found as a ratio of rebound velocity to impact velocity of the particle, Antonyuk et al. (8).

The hydrodynamics of the gas phase considered as continuum is calculated using volume-averaged Navier-Stokes equations (6)-(7).

$$\frac{\partial}{\partial t} (\varepsilon \rho_g) + \nabla \cdot (\varepsilon \rho_g \mathbf{u}_g) = 0, \quad (6)$$

$$\frac{\partial}{\partial t} (\varepsilon \rho_g \mathbf{u}_g) + \nabla \cdot (\varepsilon \rho_g \mathbf{u}_g \mathbf{u}_g) = -\varepsilon \nabla p_g - \nabla \cdot (\varepsilon \boldsymbol{\tau}_g) - \mathbf{S}_p + \varepsilon \rho_g \mathbf{g}. \quad (7)$$

Simulations were performed using the commercial simulators EDEM and Fluent.

### Simulation Parameters

The geometry of fluidization chamber (2 in Fig. 1) is discretized in mesh cells (Fig. 5). The mesh consists of 76.725 tet/hybrid cells with an interval size of 0.008 and minimum volume of 4 mm<sup>3</sup>. The air with the temperature of 25 °C, density of 1.18 kg/m<sup>3</sup> and kinematic viscosity of 15.7 · 10<sup>-6</sup> m<sup>2</sup>/s was calculated. To describe the effects of turbulent fluctuations of velocities on the pressure drop of the empty apparatus a k- $\varepsilon$  model (with the turbulence intensity of 5%) was applied for the calculation which showed good results for the spout beds in CFD simulations of Gryczka et al. (9). The parameters of the DEM model are given in Table 3.

Table 3 Properties of the particles in DEM model.

Parameter	uncoated	coated
diameter in $\mu\text{m}$	800	820
density in $\text{kg/m}^3$	190	300
stiffness in $\text{N/mm}$	10	10
shear modulus in $\text{MPa}$	6.25	6.25
restitution coefficient	0.6	0.4
friction coefficient	0.8	0.8
rolling friction coefficient	0.01	0.01
number of the particles	150.000	150.000

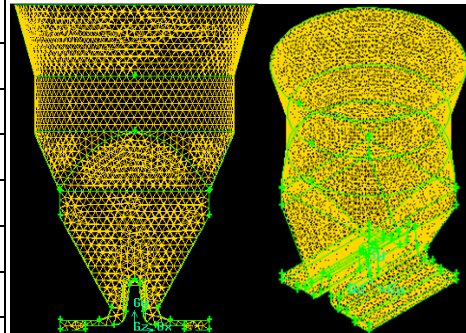


Fig. 5 Mesh of CFD simulation.

The DPM simulations were performed for the dry uncoated aerogel particles and compared with the case of coated particles. The coated particles are significantly heavier than dry uncoated aerogel. Moreover, with the wetting the energy adsorption during impact increases that results in the decreasing the coefficient of restitution (Antonyuk et al. (10)).

## SIMULATION RESULTS

First simulations were performed for the empty apparatus without the solid particles. The inlet velocity of the gas was varied in the range of 1-2 m/s. The calculated pressure drop increases with increasing inlet velocity (Fig. 6). The calculated pressure drop predicted well with the experimental measurements that were carried out for the full spout bed apparatus included its cylindrical chamber (Fig. 7). Therefore the predicted values of the pressure drop are smaller than experimental obtained pressure drops. The gas velocity reaches its maximum in the narrow vertical inlet splits (Fig. 8). This velocity in these zones increases linearly with increasing the inlet velocity (Fig. 6).

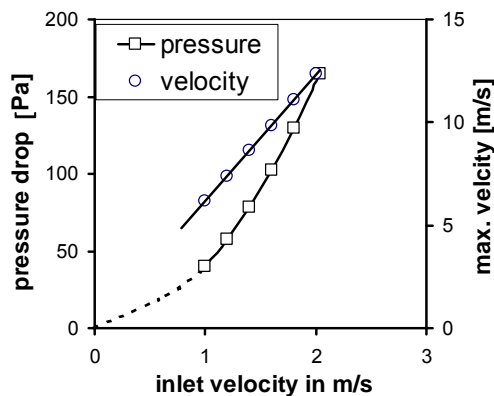


Fig. 6 Calculated pressure drop and maximum gas velocity in the empty apparatus versus the inlet gas velocity.

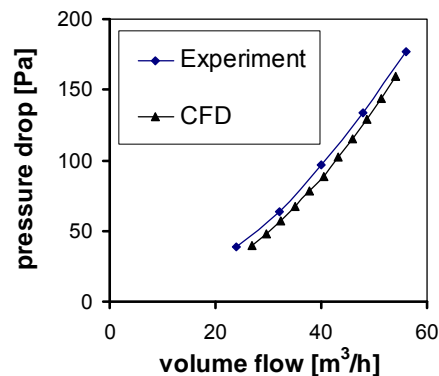


Fig. 7 Comparison of the calculated pressure drop depending on the volume flow of the inlet gas.

Fig. 8 shows the time-averaged flow profiles. The flow starts with a relatively high velocity at the bottom and becomes wider and slower with the height. Due to turbulence, two vortices are arisen that generate the secondary flow moving from the top to down in the near-wall region.

On top of the T-shaped bottom a stagnant air region takes place. The movement and drying of the particles will be reduced in this area. The particles can sink on the bottom, as shown in Fig. 9 (DPM simulation, after real fluidization time of 1.1 s). During coating experiments that leads to sticking of the particles in this region. To overcome this problem, the nozzle can be placed above this zone and the T-shaped element must be produced as knee-shaped.

Fig. 10 shows the instantaneous particle positions in the apparatus. As expected the maximum particle velocity is reached in the spout region. Here the inlet gas accelerates the particles and picks up nearly vertically according to primary flow. The gas velocity is decreased gradual over the apparatus height and leads to decreasing the particle velocity. The particles deviate from vertical air flow and moves downward along the walls. The maximum bed height depends on the gas velocity, particle mass and restitution coefficient. With increasing of the particle mass, the necessary bed height decreases. The Fig. 11 compares the calculated bed heights.

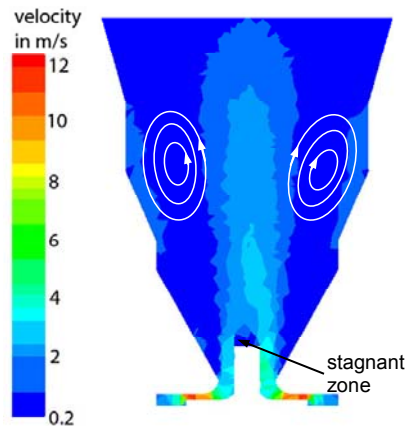


Fig. 8 The plot of time-averaged fluid velocities in the empty apparatus at the inlet velocity of 2 m/s.

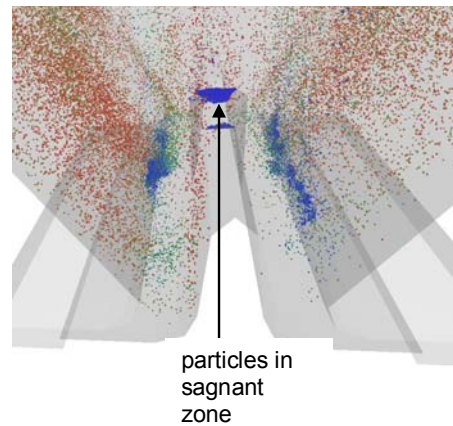


Fig. 9 The particle deposition on the middle profile in the stagnant zone of the gas (see Fig. 8).

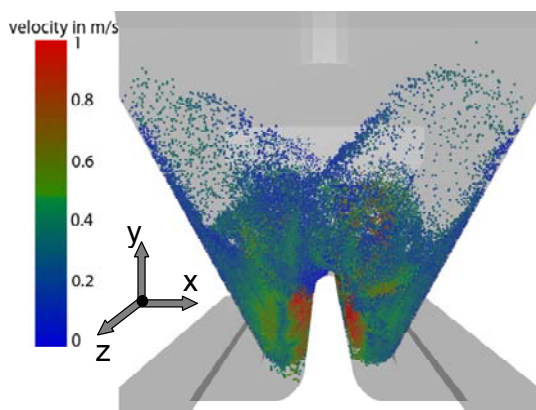


Fig. 10 Instantaneous particle positions and velocity distributions inside the spout bed apparatus (particle density =  $190 \text{ kg/m}^3$ , inlet gas velocity = 1.3 m/s).

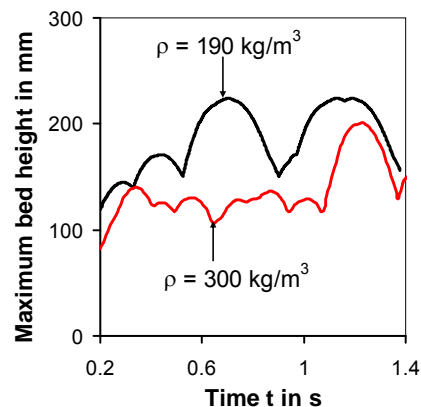


Fig. 11 Influence the particle density on the maximum bed height in the spout bed apparatus (inlet gas velocity = 1.3 m/s).

The wet coated aerogel particles showed a lower translation and rotation velocities in comparison with dry and light aerogels (Table 4). Therefore, during the coating process, the inlet gas flow and the velocity must be increased in order to keep constant particle dynamics and to avoid sticking and agglomeration. The obtained distributions of the average particle velocity and impact velocity in spouted bed can be described with a lognormal distribution function, as it shown in Fig. 12. The average particle-particle impact velocity (Fig. 12 right) is about 7 times smaller than the absolute particle velocity at the same simulation time. The mean impact velocity by particle-wall impact is at the average 15 % higher than that by impact of particles.

Table 4 Time-averaged motion parameters.

parameter	uncoated particles	coated particles
maximum bed height in mm	165	130
mean/maximum particle velocity in m/s	0.36/1.62	0.28/1.20
average particle rotation in 1/s	275	226

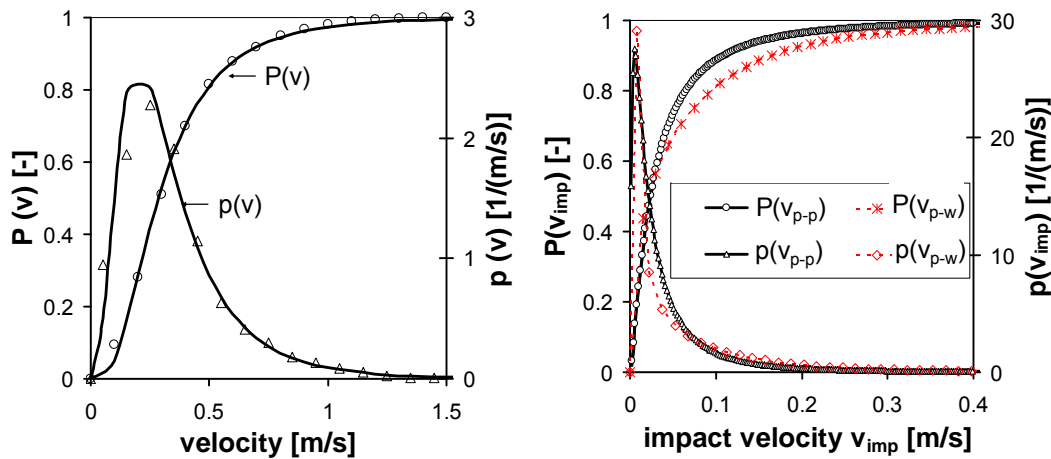


Fig. 12 Distribution function  $P$  and its density  $p$  for: (left) average absolute particle velocity and (right) relative impact velocity in the spout bed apparatus. (particle density of  $300 \text{ kg/m}^3$ ; p-p - particle-particle impacts, p-w - particle-wall impacts).

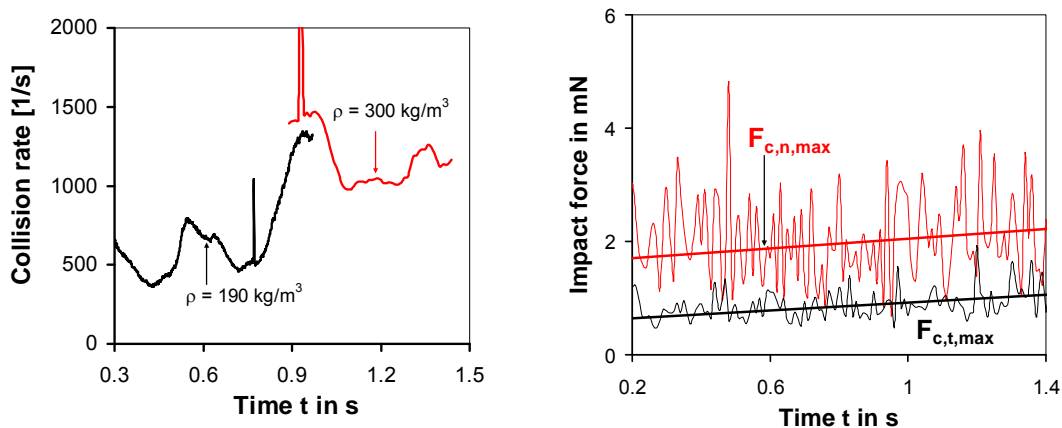


Fig. 13 (left) Collision rate of the particles during the fluidization time, (right) maximal values of the normal and tangential impact forces (particle density of  $300 \text{ kg/m}^3$ ).



Fig. 13 shows the calculated particle-particle collision rates. The fluidized bed of wetted particles shows smaller height and porosity and so higher collision rates than for dry aerogels. The particle collides with another particle almost ten times more frequently than with a wall. The calculated forces acting on the particles during collisions in the bed (Fig. 13 right) are significantly smaller than breakage range of the aerogels (Table 2). This confirms the experimental fact that no breakage occurs during fluidization of aerogels. The small magnitude of the force can be explained by relative small particle impact velocities in the presented apparatus (Fig. 12).

## CONCLUSIONS

The process of coating silica aerogels with pH sensitive polymers was performed successfully in the experimental spouted bed apparatus. To produce a closed Eudragit® layer and to avert the shrinking and breakage of the aerogel the particles can be coated with PEG 2000 as protection material.

The DPM simulations showed a high gas velocity in the bottom part of the apparatus and its gradual decrease over the apparatus. The increasing mass and energy dissipation at the contact during the coating decreases the bed height, particle velocities and increases the collisions rate. The average impact velocity in spouted bed can be described with a lognormal distribution function. No breakage of the aerogels was obtained because the impact forces acting in the fluidized bed are significantly smaller than the measured breakage force of aerogel particles.

## REFERENCES

1. Antonyuk, S., Heinrich, S., Alnaief, M. and I. Smirnova: Application of a novel spouted bed process for the drying and coating of silica aerogel microspheres for advanced drug delivery, 17th International Drying Symposium, Magdeburg, 2010.
2. Mörl, L., Heinrich, S., Peglow, M., The Macro Scale I: Processing for Granulation, in Handbook of Powder Technology, Vol. 11, Elsevier Science, (2005), 21-188.
3. Alnaief, M., Smirnova I.: In situ production of spherical aerogel microparticles, J. of Supercritical Fluids 55 (2010) 3, 1118-1123.
4. Antonyuk, S., Palis, S., Heinrich, S.: Breakage behaviour of agglomerates and crystals by static loading and impact, Powder Technology 206 (2011) 88-98.
5. van Buijtenen, M.S., Deen, N.G., Heinrich, S., Antonyuk, S. and J.A.M. Kuipers: A discrete element study of wet particle-particle interaction during granulation in a spout fluidized bed, Can. J. Chem. Eng., (2009), Vol. 9999, 1-10.
6. Fries L., Antonyuk, S., Heinrich, S., Palzer, S.: DEM-CFD modelling of a fluidized bed spray granulator, Chemical Engineering Science (2011), in Press.
7. Cundall, P.A., Strack, O.D.L., A discrete numerical model for granular assemblies. Geotechnique 29 (1979), 47-65.
8. Antonyuk, S., Heinrich, S., Tomas, J., Deen, N.G., van Buijtenen, M.S. and J.A.M. Kuipers: Energy absorption during compression and impact of dry elastic-plastic spherical granules, Granular Matter 12 (2010) (1), 15-47.
9. Gryczka, O., Heinrich, S., Deen, N. van Sint Annaland, M., Kuipers, J.A.M. and L. Mörl: CFD-modeling of a prismatic spouted bed with two adjustable gas inlets, Can. J. Chem. Eng. 87 (2009), 318-328.
10. Antonyuk, S., Heinrich, S., Deen, N.G. and J.A.M. Kuipers: Influence of liquid layers on energy absorption during particle impact, Particuology 7 (2009), 245-259.